



TAPHOFACIES OF COASTAL LAKES BASED ON MOLLUSK DEATH ASSEMBLAGES: A CASE STUDY OF MIRIM LAKE

HUGO SCHMIDT-NETO

Programa de Pós-Graduação em Geologia, Universidade Vale do Rio dos Sinos, UNISINOS,
Av. Unisinos, 950, 93022-000, São Leopoldo, RS, Brazil. paleonetto@gmail.com

ABSTRACT – Mirim Lake is the second-largest lacustrine body in Brazil, stretching for some 185 km and covering about 375 thousand hectares of water surface. This lake is part of the Patos-Mirim System, one of the world’s largest complexes of coastal lagoons, which is the result of the rise and fall of sea level over transgressive-regressive cycles triggered by glacio-eustasy during the Late Pleistocene and Holocene. Its characteristics and dynamics give it singular importance for studies on the genesis of shell accumulation in lagoons. This study aims to improve the knowledge of how the taphonomic signatures reflect the environmental characteristics and dynamics of Mirim Lake. Categorization of the arrangement and packing of death assemblages, as well as the orientation of shells, supported the biostratigraphical approach. The taphonomic signatures included disarticulation, fragmentation, and corrosion of shells. Corrosion is the primary damage observed in the bioclasts, varying from a single loss of color to complete degradation. Differences in the characteristics of death assemblages observed in the dune fields and the lacustrine plain led to the recognition of two taphofacies. A more significant number of whole shells was observed in the dune field taphofacies, while sharp fragments and open-articulated bivalves in hydrodynamic unstable positions characterize the lacustrine plain taphofacies. The genesis of death assemblages and the taphonomic signatures of bioclasts were linked to three sedimentary dynamics attributed to the environment of Mirim Lake.

Keywords: biostratigraphy, taphonomic signatures, shell deposits, dune field, lacustrine plain.

RESUMO – A Lagoa Mirim é o segundo maior corpo lacustre do Brasil, estendendo-se por cerca de 185 km e cobrindo cerca de 375 mil hectares de superfície de água. Este lago faz parte do Sistema Patos-Mirim, um dos maiores complexos de lagoas costeiras do mundo, que é o resultado da subida e descida do nível do mar ao longo de ciclos transgressivos-regressivos desencadeados pela glacio-eustasia durante o Pleistoceno Superior e o Holoceno. Suas características e dinâmica lhe conferem importância singular para estudos sobre a gênese do acúmulo de conchas em lagoas. Este estudo visa aprimorar o conhecimento de como as assinaturas tafonômicas refletem as características e dinâmicas ambientais da Lagoa Mirim. A bioestratigrafia dos depósitos foi embasada no arranjo e empacotamento das assembleias mortas, bem como na orientação das conchas. Entre as assinaturas tafonômicas destacam-se a desarticulação, a fragmentação e a corrosão das conchas. A corrosão é o principal dano observado nos bioclastos, variando desde a perda da cor até a degradação completa da concha. Diferenças nas características das associações de mortas observadas nos campos de dunas e na planície lacustre levaram ao reconhecimento de duas tafofácies. Um número mais significativo de conchas inteiras foi observado nas tafofácies do campo de duna, enquanto fragmentos pontiagudos e conchas articuladas e abertas, em posições hidrodinâmicas instáveis, caracterizam as tafofácies da planície lacustre. A gênese das associações mortas e as assinaturas tafonômicas dos bioclastos foram relacionadas a três dinâmicas sedimentares atribuídas ao ambiente da Lagoa Mirim.

Palavras-chave: bioestratigrafia, assinaturas tafonômicas, depósitos de conchas, campo de dunas, planície lacustre.

INTRODUCTION

The characteristics of shell deposits intrinsically depend on environmental dynamics (Brett & Baird, 1986; Kidwell *et al.*, 1986; Speyer & Brett, 1988; Fürsich & Oschmann, 1993; Tsolakos *et al.*, 2021), which led taphonomists to develop research with fossil assemblages from marine and continental environments (Kidwell & Jablonski, 1983; Brett & Baird, 1986; Fürsich & Kirkland, 1986; Kidwell, 1986; Speyer & Brett, 1988; Fürsich & Oschmann, 1993; Kidwell, 1998, 2001, 2013; Best & Kidwell, 2000a; Behrensmeier *et al.*, 2005; Fürsich *et al.*, 2016; Tsolakos *et al.*, 2021). Based on the intrinsic relation between environmental dynamics

and the genesis of the bioclast concentrations, Speyer & Brett (1986, 1988) proposed the concept of a taphofacies model for epeiric seas (*i.e.*, a link between sedimentary dynamic and taphonomic signatures present in the fossil deposits). This concept has become prevalent in the taphonomic research aimed at interpreting environmental dynamics.

To improve the knowledge of sedimentary dynamics related to biostratigraphy, a branch of paleontology (actuo-paleontology) has emerged, and paleontologists have been focusing on modern analogs to understand the past (*e.g.*, Meldahl, 1987; Meldahl & Flessa, 1990; Kowalewski *et al.*, 1994; Kowalewski, 1999; Best & Kidwell, 2000a, b; Kidwell, 2008). These types of studies have proven central to ecological

and paleoecological research (Kowalewski, 1999; Kidwell, 2007, 2008, 2013; Dietl & Flessa, 2011; Weber & Zuschin, 2013; Zuschin & Ebner, 2015; Dietl, 2016), and it is essential to apply them to as many modern and varied environments as possible. Investigations on freshwater and estuarine environments also bring significant contributions to taphonomic studies. For instance, in Brazil, Ghilardi & Simões (2002) studied the taphonomic signatures associated with freshwater bivalves to improve paleoenvironmental and paleoecological interpretations of the Passa Dois Formation (Late Permian).

Extending for some 185 km and covering about 375 thousand hectares of water surface, Mirim Lake (Figure 1A) is the second-largest lacustrine body in Brazil (Oliveira *et al.*, 2015; Valentini *et al.*, 2020; Lopes *et al.*, 2021), which gives it singular importance for the study of the genesis of shell accumulations in freshwater bodies. This lake is part of one of the world's largest complexes of coastal lakes and lagoons, the Patos-Mirim System, which consists of Patos Lagoon, Mirim Lake, Mangueira Lake, and smaller lakes and marshes (see Lopes *et al.*, 2021). This extensive complex results from the rise and fall of sea level along the transgressive-regressive cycles triggered by glacio-eustasy during the Pleistocene and Holocene.

During the transition from the Late Pleistocene (*ca.* 325 ka to 125 ka) to the Early Holocene (*ca.* 8 ka), the landscape was flooded by marine transgression, and four barriers were formed (Figure 1B) (Rosa *et al.*, 2017). Afterward, the following regression resulted in the formation of the lakes and lagoons in the back-barrier zone (Figure 1A) (Villwock & Tomazelli, 1995; Tomazelli & Villwock, 2000; Rosa *et al.*, 2017). Consequently, observing fossils and modern marine and freshwater mollusks in death assemblages of lakes and lagoons is possible. Also, a complex deposit containing fossils of continental mammals along with marine mollusks has already been documented by Lopes & Buchmann (2008) from Passo da Lagoa. These characteristics make such deposits a singular window to observe the taphonomic bias on the bioclastic accumulations of large lakes of coastal plains that arise after the sea level falls.

Research on the taphonomy of mollusk bioclasts in lagoonal environments is not new (Fürsich & Kirkland, 1986; De Francesco & Hassan, 2008; Ritter *et al.*, 2013; Zuschin & Ebner, 2015; Fürsich *et al.*, 2016; Tsolakos *et al.*, 2021). In addition, the taphonomic studies conducted on coastal lagoons and lakes are relevant to improving our knowledge about mollusk diversity, taphonomy, and life history.

Mirim Lake has a beach profile comprising a well-developed dune field and a lacustrine plain (Figures 1C and D). Due to the changes in the sedimentary dynamic along the beach profile, differences in the taphonomic signatures of bioclasts are expected to be observed, leading to the recognition of different taphofacies. Thus, this study aims to understand how the taphonomic signatures reflect the environmental characteristics and dynamics of Mirim Lake and to characterize the taphofacies of this lake. Death assemblages observed on the lacustrine plain and the dune

fields of Mirim Lake were studied to fulfill this objective. Based on the distinction of taphonomic signatures along Mirim Lake, the classification of the shell deposits into taphofacies models is proposed herein.

MATERIAL AND METHODS

Field data and samples were obtained in October 2022 as a part of an undergraduate field trip in Capilha Beach (Figure 1). Mollusk death assemblages (DAs) were sampled in the lacustrine plain and the dune field (Figures 1C and D). Eight square kilometers were surveyed to record, characterize, and photograph the DAs.

A total of 4,333 mollusk bioclasts from thirteen DAs arranged in the lacustrine plain and the dune field were studied. DAs were described according to their shape (*e.g.*, narrow, broad, wavy, straight) and concentration of the shell accumulations (*e.g.*, densely to loosely concentrated, scattered accumulations). Taphonomic analysis was carried out by surveying the following signatures: fragmentation degree (whole, fragmented); articulation of bivalves (closed-articulated, open-articulated, disarticulated); orientation of valve axis in plain view (*i.e.*, unimodal, bimodal, randomly oriented); hydraulic stability of bivalve valves (*e.g.*, convex/concave upward); dissolution, bioerosion, and encrustation on bivalve valves. The bioclasts were qualified as whole (more than 90% of the valve preserved) and fragmented (less than 90% preserved). Fragments were classified as sharp or abraded (rounded). Corrosion was assessed only on bivalves and classified as initial (loss of luster, color, and minor corrosion of the surface), moderate (surface partially corroded), and severe (complete dissolution of external layers, full corrosion of umbo, exposure of the pearly layer).

To determine the azimuth orientation, the longest axis of the bioclasts was directed using a semicircular protractor. The angles were recorded in a Microsoft Excel spreadsheet. Two hydrodynamic shapes, triangular and elliptical, were recognized and used to measure the orientation of bioclasts. For bioclasts with elliptical shapes, the data were mirrored at the opposite angle to that observed in the protractor (*e.g.*, 90°–270°). Lastly, rose graphs were made to illustrate the axis direction of the bioclasts.

A Motorola Moto g31 cell phone photographed the DAs in the field. In the laboratory, a digital camera, Canon EOS Rebel XT, with a lens of 100 mm, was used to take photographs of the specimens. A few shells were sampled in the lacustrine plain and the dune field to record the taxa present in the DAs and take photos of taphonomic signatures observed in the bioclasts.

All taphonomic data from 13 DA samples were pooled into a Microsoft Excel spreadsheet for preview and general analysis. The comparison between the type of sedimentary environment (lacustrine plain and the dune field) and the state of each taphonomic signature were assessed using contingency tables (Zar, 2010). The difference in the taphonomic data for each portion (*i.e.*, the dune field and

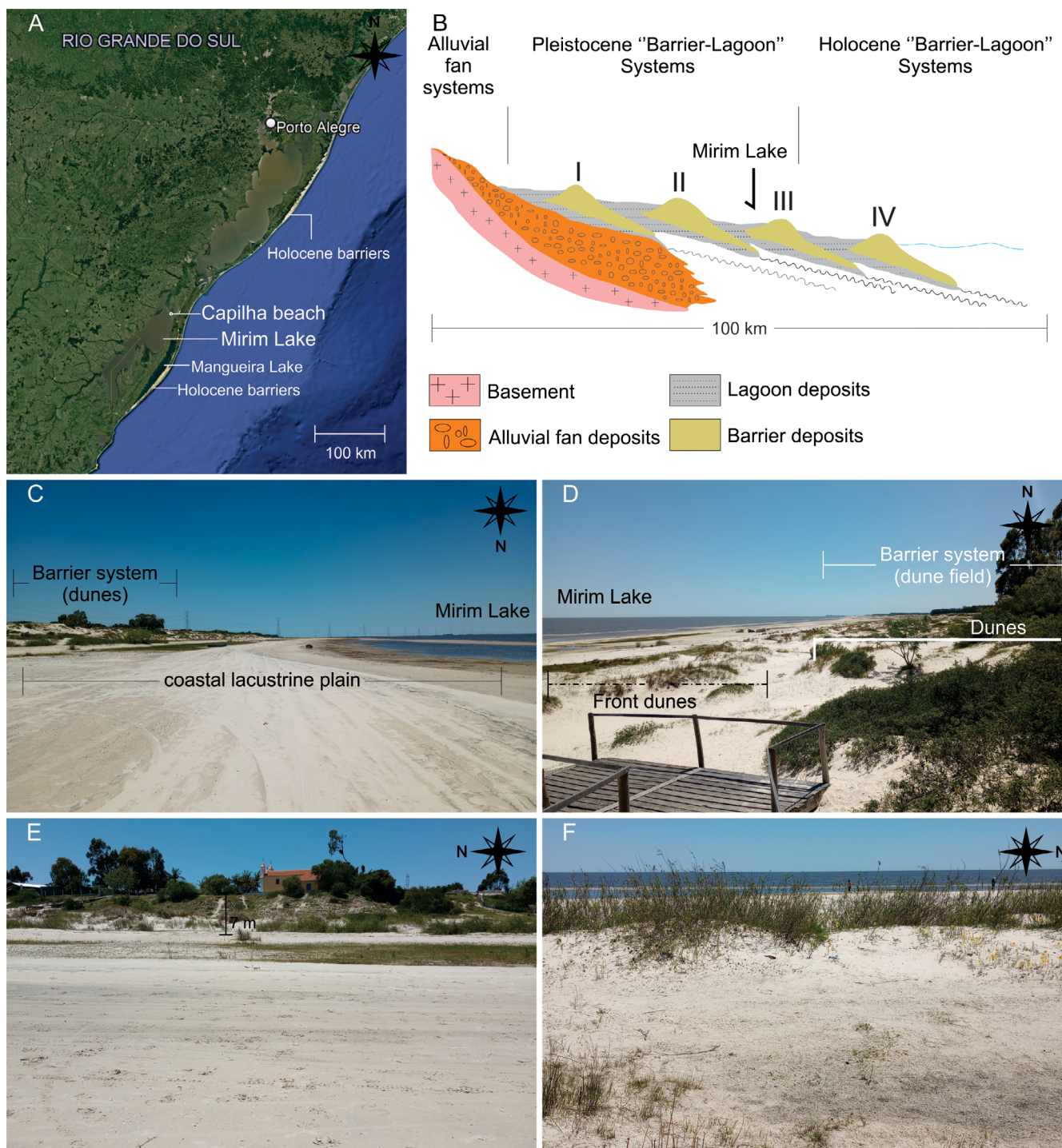


Figure 1. Map of the location of Mirim Lake and characteristics of the study area. **A**, Google Earth© image of the Patos-Mirim System and location of Capilha Beach at Mirim Lake. **B**, schematic profile of the barrier system of the Coastal Plain of Rio Grande do Sul (CPRS) with ages from systems I to IV. Adapted from Tomazelli & Villwock (2000). The black arrow indicates the relative location of Mirim Lake concerning the current Barrier-Lagoon System IV. **C**, shore of Mirim Lake delimiting the lake, lacustrine plain, and barrier system (dune field). **D** is a barrier system subdivision represented by dune fields (front dunes and dunes). **E**, frontal view of a 7-m-high dune. **F**, vegetated and non-vegetated areas of the dune field.

lacustrine plain) of the Mirim Lake was used as a criterion to separate them into distinct taphofacies. Moreover, differences in the results observed in vegetated and non-vegetated zones of the dune field were also noted, which led to the proposal of sub-taphofacies to represent each one.

Taxonomic data were adjusted to available information on the online platforms Paleobiology Database (<https://paleobiodb.org/>), WORMS (<https://www.marinespecies.org/>), MolluscaBase (<https://www.molluscabase.org/>), and SiBBR (<https://sibbr.gov.br/>).

The samples collected were deposited in the Museu da História da Vida e da Terra of the Universidade do Vale do Rio dos Sinos (Unisinos), São Leopoldo, Brazil. They were identified by initial ULVG followed by the ID number in the collection.

GEOLOGICAL SETTING AND THE STUDY AREA

The Pelotas Basin is located in the southernmost continental margins of Brazil and Uruguay. It is characterized as a subsided marginal and open basin filled with continental and marginal marine sediments (Barboza *et al.*, 2008). Its genesis is related to the erosion of Precambrian, Paleozoic, and Mesozoic rocks after the opening of the Atlantic Ocean, with sediment accumulation between the Cretaceous and the Quaternary periods (Villwock & Tomazelli, 1995; Barboza *et al.*, 2008). In their onshore portion, two depositional systems represented by alluvial fans and barrier-lagoon deposits are identified (Figure 1B). Alluvial fan deposits are considered Miocene age, while barrier-lagoon systems developed in the Quaternary (Tomazelli & Villwock, 2005). The transgressive-regressive events that reworked the alluvial fan system also generated the four Quaternary-aged barrier-lagoon depositional systems that have been developed and shaped by high-frequency, 4th order (100 ka) glacio-eustatic cycles (Villwock & Tomazelli, 1995; Tomazelli & Villwock, 2005; Rosa *et al.*, 2017; Lopes *et al.*, 2020). Each barrier was probably formed during the transgression and preserved by forced shoreline regression (Tomazelli & Villwock, 2005).

Three sets of depositional sequences (*i.e.*, progradational-aggradational, retrogradational, and progradational-degradational) were proposed by Rosa *et al.* (2017) as a result of transgressive-regressive pulses that formed the barrier-lagoon system of the Coastal Plain of the state of Rio Grande do Sul (CPRS). The barrier-lagoon systems have been developed parallel to each other, following the coastline orientation. These include long sand barriers extending for more than 600 km, lagoons, lakes, and wetlands arranged on the back-barrier zone (Figure 1A). Their deposits are represented by the shallow marine and eolian sand facies (*e.g.*, barriers) and mud facies of the bottom of lagoons and coastal lakes. Siliciclastic, fine to very fine-grained sands, with small amounts of feldspars, biogenic carbonates (from shell degradation), and heavy minerals characterize the sediments of barriers (Lopes *et al.*, 2020).

The Mirim Lake originated in the marine transgression of the Middle Holocene and became a brackish lagoon about 7.6 ka ago. However, it had a fully saltwater condition *ca.* 6–5 ka ago during the sea-level highstand, and the marine influence reduced *ca.* 4 ka ago with the fall of the sea level and closure of the connection with the ocean after the evolution of the sand barrier that originated the current shoreline (Lopes *et al.*, 2021).

At the margin of the Mirim Lake, sand barriers are present as dunes covered by typical shoreline plants (Figures 1D–F). Bivalve and gastropod shells are found along the beach profile

(*ca.* 180 m of extension), with the shell deposits occurring from the lacustrine plain to the front dunes (Figures 1C and D). The dune fields are about 117 m distant from the lake, widespread parallel to the coast, and reach around 7 m above the lake level (Figures 1E). Mollusk and vertebrate fossils have been reported in several marginal zones, occurring at a few centimeters down in the subsurface or on the surface as exhumed materials (Lopes *et al.*, 2021, references therein).

RESULTS

A total of 4,333 bioclasts arranged into 13 DAs were observed along the dune field and the lacustrine plain of Mirim Lake. They were arranged as scattered, loosely, and densely concentrated shell deposits (Figures 2 and 3). Of these, 57.44% of the bioclasts were whole ($n = 2,489$), 7.6% were abraded fragments ($n = 532$), and 27% were sharp fragments ($n = 1,312$). Many bioclasts identified as *Corbicula fluminea* Müller, 1774 showed a pattern of fragmentation irradiating from the center to the margin of the valve (Figure 2D); 8.7% of all bioclasts ($n = 379$) were articulated (closed = 7.4%, open = 1.3%; Figures 2C and F), and 35.5% of convex bioclasts ($n = 644$) were oriented in a hydrodynamic unstable position (Figure 2C); 87% of bioclasts ($n = 3,756$) showed initial stages of corrosion, while bioclasts with no damage ($n = 275$) and moderate damage ($n = 249$) corresponded to 6% each. Severe corrosion damage was observed in 1% of bioclasts ($n = 53$). A synthesis of the distribution of bioclasts according to the taphonomic variables is shown in Table 1.

Six bivalve taxa (*Corbicula fluminea* Müller, 1744, *Corbicula cf. lacustris* Martens, 1897; *Corbicula* sp., *Erodona mactroides* Bosc, 1801, *Diplodon ellipticus* Spix, 1827, *Limnoperna fortunei* Dunker, 1857), and one gastropod species (Cochliopidae Tryon, 1866) were identified as components of DAs (Figures 2E, and 4F). Golden mussels (*L. fortunei*) occurred as gregarious elements along the shore (Figure 4F), and local accumulations of Cochliopidae were observed in the DAs (Figure 2E).

Five DAs ($n = 2,949$, 68% of the bioclasts) were recorded in the lacustrine plain, while eight DAs ($n = 1,384$, 32% of the bioclasts) were recorded in the dune field. Dense concentrations of shell accumulations were recorded only in the vegetated portions of the dune field. In non-vegetated areas of the dune field and the lacustrine plain, the shell deposits were arranged as scattered and loose concentrations (Figures 2B and 3). Concerning taphonomic variables, the dune field and lacustrine plain taphofacies are recognized, differing from each other in all taphonomic signatures evaluated (Table 1, Figure 5).

Dune field taphofacies (front dune zone)

In the dune field taphofacies, the wind is the most effective agent in the transportation and remobilization of sediments (Tomazelli, 1993). This environment is subdivided into dunes and front dunes (Figure 1D). Front dunes are characterized by vegetated and non-vegetated areas (Figure 1F). The DAs were observed in this zone of the dune fields.

Table 1. Relative abundance of taphonomic signatures of the lacustrine plain and the dune field taphofacies and result of chi-square (χ^2) test to similarity for each category. Chi-square significance: if $p \geq 0.05$ = no significant difference; if $p < 0.05$ = considerable difference.

Taphonomic signatures	Lacustrine plain		Dune field		Chi-square significance values
	Observed data	Expected data	Observed data	Expected data	
Fragmentation					
Whole	1,449	1,694	1,040	795	$\chi^2 = 388.97$ $p < 0.0001$
Abraded fragment	330	362	202	170	
Sharp-edged fragment	1,170	893	142	419	
Whole	1,449	1,694	1,040	795	$\chi^2 = 260.66$ $p < 0.0001$ (with Yates' continuity correction)
Fragmented	1,500	1,255	344	589	
Abraded fragment	330	433	202	99	
Sharp-edged fragment	1,170	1,067	142	245	$\chi^2 = 182.04$ $p < 0.0001$ (with Yates' continuity correction)
Articulation					
Close-articulated	68	220	255	103	$\chi^2 = 368.32$ $p < 0.0001$
Open-articulated	53	38	3	18	
Disarticulated	2,828	2,691	1,126	1,263	
Close-articulated	68	103	255	220	$\chi^2 = 115.56$ $p < 0.0001$ (with Yates' continuity correction)
Open-articulated	53	18	3	38	
Articulated	121	258	258	121	$\chi^2 = 247.62$ $p < 0.0001$ (with Yates' continuity correction)
Disarticulated	2,828	2,691	1,126	1,263	
Hydraulic stability					
Stable (convex up)	1,132	1,063	409	478	$\chi^2 = 48.511$ $p < 0.0001$ (with Yates' continuity correction)
Unstable (convex down)	375	444	269	200	
Dissolution					
No	60	187	215	88	$\chi^2 = 286.55$ $p < 0.0001$
Corroded	2,889	2,762	1,169	1,296	
Initial	2,744	2,556	1,012	1,200	
Moderate	127	169	122	80	$\chi^2 = 91.667$ $p < 0.0001$
Severe	18	36	35	17	

Shell accumulations formed patches of densely to loosely concentrated and scattered shapeless shell deposits (Figures 2A and B). Whole bioclasts are more abundant than fragments ($p < 0.0001$) and totalize 75% of the sample ($n = 1,040$ of 1,384) (Table 1, Figure 5A). The ratio between abraded and sharp-edged fragments is significantly lower than in the lacustrine plain taphofacies ($p < 0.0001$) (Table 1). In contrast, the frequency of articulated shells and the subcategories of open and closed-articulated shells were significantly higher ($p < 0.0001$). A total of 258 articulated valves, between close ($n = 255$) and open ($n = 3$), were recorded in the dune field taphofacies (Figure 5B, Table 1).

Inspection of the plot of Figure 6A does not allow for the recognition of any preferential orientation of shells in the plan view. A total of 269 valves ($f = 20\%$) were oriented in a hydraulic unstable position and are significantly different from the lacustrine plain taphofacies ($p < 0.0001$) (Figure 5C, Table 1). Corrosion classified as initial was recorded in 73% ($n = 1,012$) of the bioclasts, while 16% ($n = 215$ of 1,384) did not exhibit signs of dissolution (Figure 5D, Table 1).

The taphonomic data from two areas of the front dunes (*i.e.*, vegetated and non-vegetated dune fields) were significantly different in almost all taphonomic signatures (Figure 7, Table 2). Non-vegetated dune-field sub-taphofacies



Figure 2. Field photographs of death assemblages in the dune field and lacustrine plain. **A**, densely to loosely concentrated death assemblage forms patches in vegetated front dunes (dune field taphofacies). **B**, scattered shell deposits in the non-vegetated area of the front dune zone (dune field taphofacies). **C**, shells scattered in the lacustrine plain with open-articulated bivalves (**op. art.**). **D**, loosely concentrated death assemblage from the lacustrine plain composed of whole and fragmented bioclasts and trampled valves (**tra.**). **E**, local gastropods (**G**) accumulation in the dune field taphofacies. **F**, scattered closed-articulated bivalves (**clos. art.**) deposited in the dune field taphofacies. **C**, **D**, and **F**, monospecific death assemblages composed of *Corbicula fluminea*; **E**, gastropod shells were identified as Cochliopidae. Not scale.

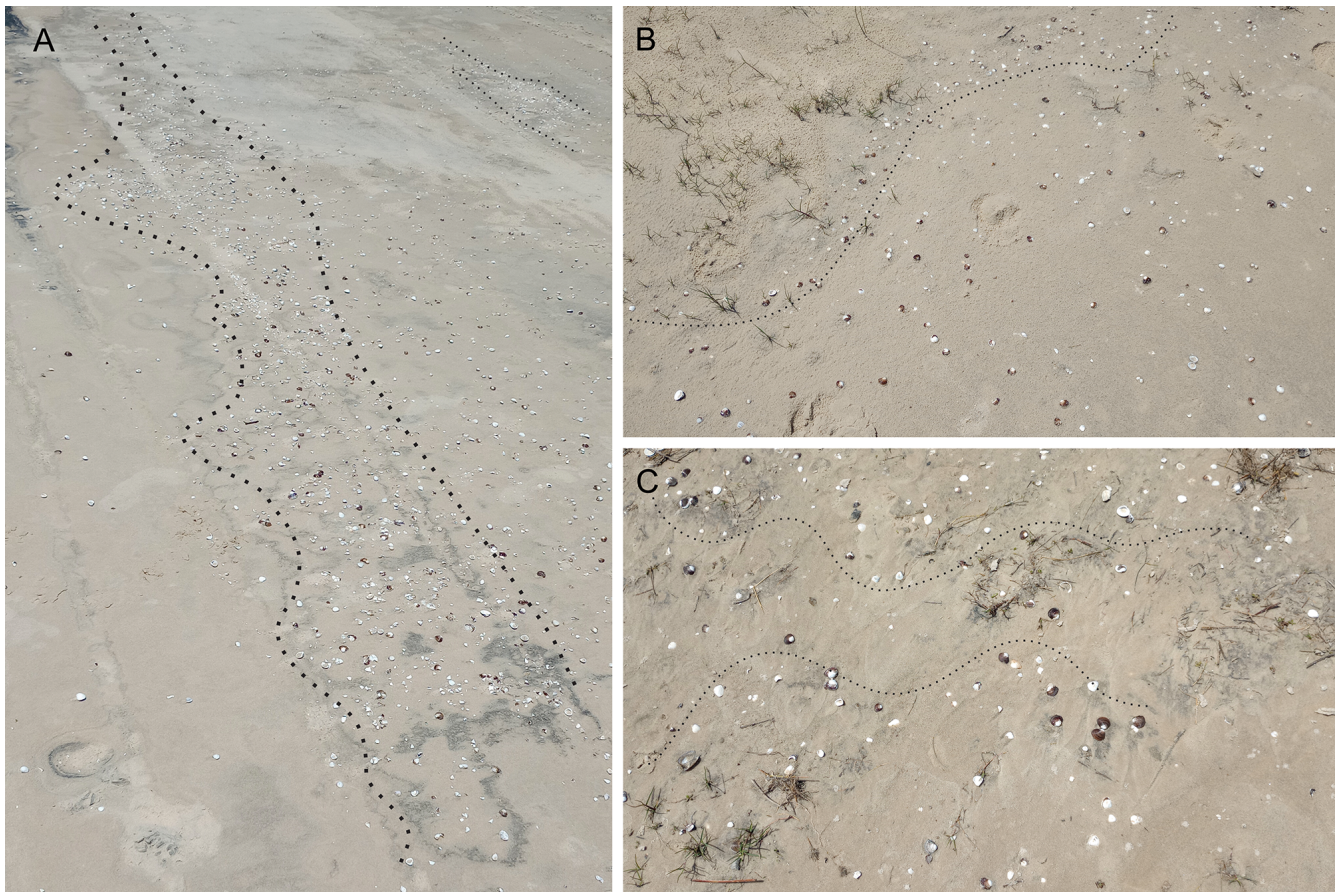


Figure 3. Geometry characterization of death assemblages in the lacustrine plain taphofacies. **A**, loosely packed concentration showing string geometry. **B** and **C**, scattered deposits. The dotted line indicates the wavy arrangement observed in the death assemblages of the lacustrine plain produced by wave reworking. Not scale.

show a higher percentage of valves in hydrodynamically stable than unstable positions ($p < 0.0001$). Based on these data, the classification of the dune field taphofacies into two sub-taphofacies was proposed. A description of each sub-taphofacies is presented below.

Vegetated dune field sub-taphofacies

Vegetated dunes show higher percentages of abraded than sharp-edged bioclasts ($p < 0.0001$) (Figure 7A). Among the total of 245 fragments, 68% ($n = 167$) are abraded, and 32% ($n = 78$) are sharp-edged (Table 2). However, the two sub-taphofacies do not differ regarding the whole/fragmented ratio ($p = 0.148$). A higher proportion of articulated than disarticulated shells ($p < 0.0001$) was recorded in vegetated dunes (Figure 7B). Disarticulated shells represent 85% ($n = 799$) of the total bioclasts from vegetated dunes (Figure 7C). Nevertheless, the open/closed-articulated ratio is not significantly different ($p = 0.13$). In the vegetated dunes, a higher frequency of convex bioclasts in a hydrodynamic unstable position was observed ($p < 0.0001$) (Figure 7D). Corrosion of bioclasts is more frequent in vegetated than in non-vegetated dunes ($p = 0.005$) (Figure 7E). Among corroded bioclasts, 88% ($n = 806$ of the 913) were qualified as initially damaged (Figure 7F, Table 2).

This sub-taphofacies is covered by herbaceous vegetation of the *Restinga* ecotone (Figures 1D–F). Dense to loosely concentrated shell deposits occurred among the vegetation (Figure 2A). A total of 68% ($n = 940$ of 1,384) of the bioclasts were observed in this part of the dune field (Table 2).

Non-vegetated dune field sub-taphofacies.

Of the 444 bioclasts from non-vegetated dunes, 99 were fragments, of which 35 were abraded ($f = 35\%$), and 64 were sharp-edged ($f = 65\%$) (Table 2). In non-vegetated dunes, a higher frequency of sharp-edged fragments was observed ($p = 0.0001$) (Figure 7A), 327 ($f = 74\%$) of the bioclasts were disarticulated (Table 2). However, the frequency of articulated shells in non-vegetated dunes is significantly higher than that observed in vegetated dunes ($p = 0.0001$) (Figure 7C). A higher frequency of valves in a hydrodynamic stable position ($n = 114$ of the 145, $f = 79\%$) is recorded in non-vegetated dunes ($p < 0.0001$) (Figure 7D); 42% ($n = 188$ of the 444) did not exhibit corrosion signs ($p < 0.0001$) (Figure 7E). The frequency of corroded bioclasts is lower than in vegetated dunes ($p < 0.0001$) (Figures 7E and F, Table 2).

In addition, sub-taphofacies of non-vegetated dunes correspond to paths devoid of vegetation that intersect the

Table 2. Relative abundance of taphonomic signatures of the vegetated and non-vegetated sub-taphofacies of the dune field and the result of chi-square (χ^2) test to similarity for each category. Chi-square significance: if $p \geq 0.05$ = no significant difference; if $p < 0.05$ = significant difference.

Taphonomic signatures	Vegetated dune		Non-vegetated dune		Chi-square significance
	Observed data	Expected data	Observed data	Expected data	
Fragmentation					
Whole	695	706	345	334	$\chi^2 = 31.746$ $p < 0.0001$
Abraded fragment	167	137	35	65	
Sharp-edged fragment	78	96	64	46	
Whole	695	706	345	334	$\chi^2 = 2.0933$ $p = 0.1479$ (with Yates' continuity correction)
Fragmented	245	234	99	110	
Abraded fragment	167	144	35	58	
Sharp-edged fragment	78	101	64	41	$\chi^2 = 29.974$ $p < 0.0001$ (with Yates' continuity correction)
Articulation					
Closed-articulated	138	139	117	115	$\chi^2 = 28.485$ $p < 0.0001$
Open-articulated	3	2	0	2	
Disarticulated	799	765	327	361	
Closed-articulated	138	139	117	115	$\chi^2 = 2.24$ $p = 0.13$ (with Yates' continuity correction)
Open-articulated	3	2	0	2	
Articulated	141	175	117	83	$\chi^2 = 24.877$ $p < 0.0001$ (with Yates' continuity correction)
Disarticulated	799	765	327	361	
Hydraulic stability					
Stable (convex up)	295	322	114	87	$\chi^2 = 24.834$ $p < 0.0001$ (with Yates' continuity correction)
Unstable (convex down)	238	211	31	58	
Corrosion					
No	27	146	188	69	$\chi^2 = 355.0373$ $p < 0.0001$ (with Yates' continuity correction)
Corroded	913	794	256	375	
Initial	806	687	206	325	$\chi^2 = 10.498$ $p = 0.0052$
Moderate	83	83	39	39	
Severe	24	24	11	11	

vegetated areas of the front dunes (Figure 1F), with dispersed to scattered shapeless shell deposits.

Lacustrine plain taphofacies

The lacustrine plain is an emerged, flat, and smoothly sloped sand portion of the lake closer to the water body (Figure 1C). In this zone of the lake, the shell deposits were distributed as narrow and laterally elongated accumulations forming a sinuous string geometry (Figure 3). In these DAs, bioclasts were arranged as loose concentrations and scattered shapeless shell deposits (Figures 3A–C).

Higher levels of disarticulation ($p < 0.0001$) and fragmentation ($p < 0.0001$) were observed in the lacustrine plain. Of the fragments, 1500 were less abraded than sharp-

edged ($p < 0.0001$), 330 fragments were abraded ($f = 22\%$), and 1170 were sharp-edged ($f = 78\%$) (Table 1). Convex-up bioclasts were more frequently observed in the coastal plain taphofacies ($p < 0.0001$) (Table 1); 121 (4%) valves were articulated, of which 68 ($f = 56\%$) were closed, and 53 ($f = 44\%$) were open (Table 1). Open-articulated shells are more abundant in this part of the lake ($p < 0.0001$).

As observed in the dune field, the inspection of Figure 6B does not allow for the recognition of any preferential orientation of bioclasts. One thousand one hundred thirty-two convex bioclasts ($f = 75\%$) were oriented in a hydrodynamic stable position (Figure 5C, Table 1). The rate of convex-up valves in the lacustrine plain is significantly higher than in the dune fields ($p < 0.0001$) (Table 1). Of the 2949 bioclasts, 2889

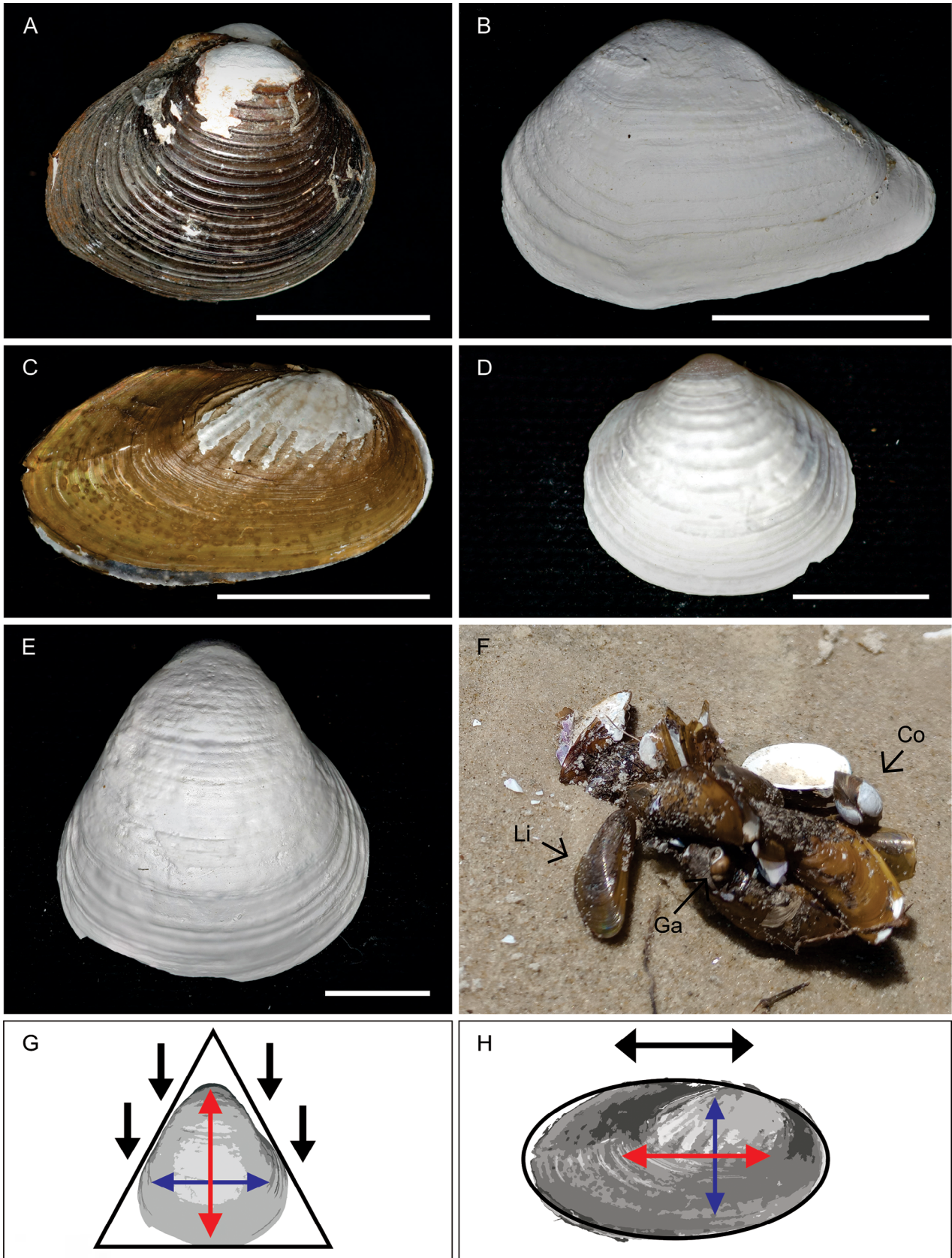


Figure 4. Bivalve taxa are present in the death assemblages. **A**, *Corbicula fluminea* (ULVG 14291). **B**, *Erodona mactroides* (ULVG 14301). **C**, *Diplodon ellipticus* (ULVG 14304). **D**, *Corbicula* sp. (ULVG 14306). **E**, *Corbicula* cf. *lacustris* (ULVG 14308). **F**, gregarious golden mussel *Limnoperna fortunei* (Li), one specimen of gastropoda Cochliopidae (Ga), and one closed-articulated *Corbicula fluminea* (Co). **G–H**, schematic drawing to illustrate the triangular (**G**) and elliptical (**H**) shapes. The black arrows in G and H indicate the current direction. Red arrows point to the long axis, while blue arrows point to the short axis of each morphology. Scale bars = 10 mm

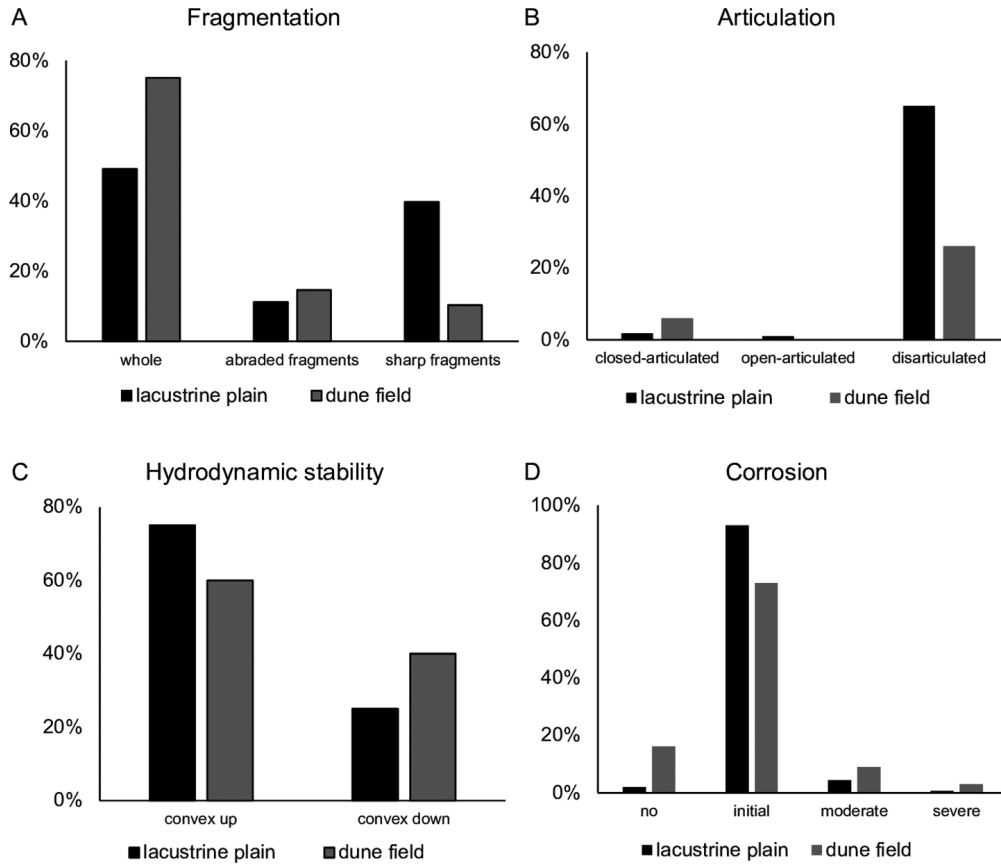


Figure 5. The relative frequency of taphonomic signatures observed in the lacustrine plain and the dune field. **A**, Fragmentation. **B**, Articulation. **C**, Hydrodynamic stability of convex valves related to the bottom. Convex up = stable hydrodynamic position, convex down = unstable hydrodynamic position. **D**, Corrosion (see Material and Methods for damage categories).

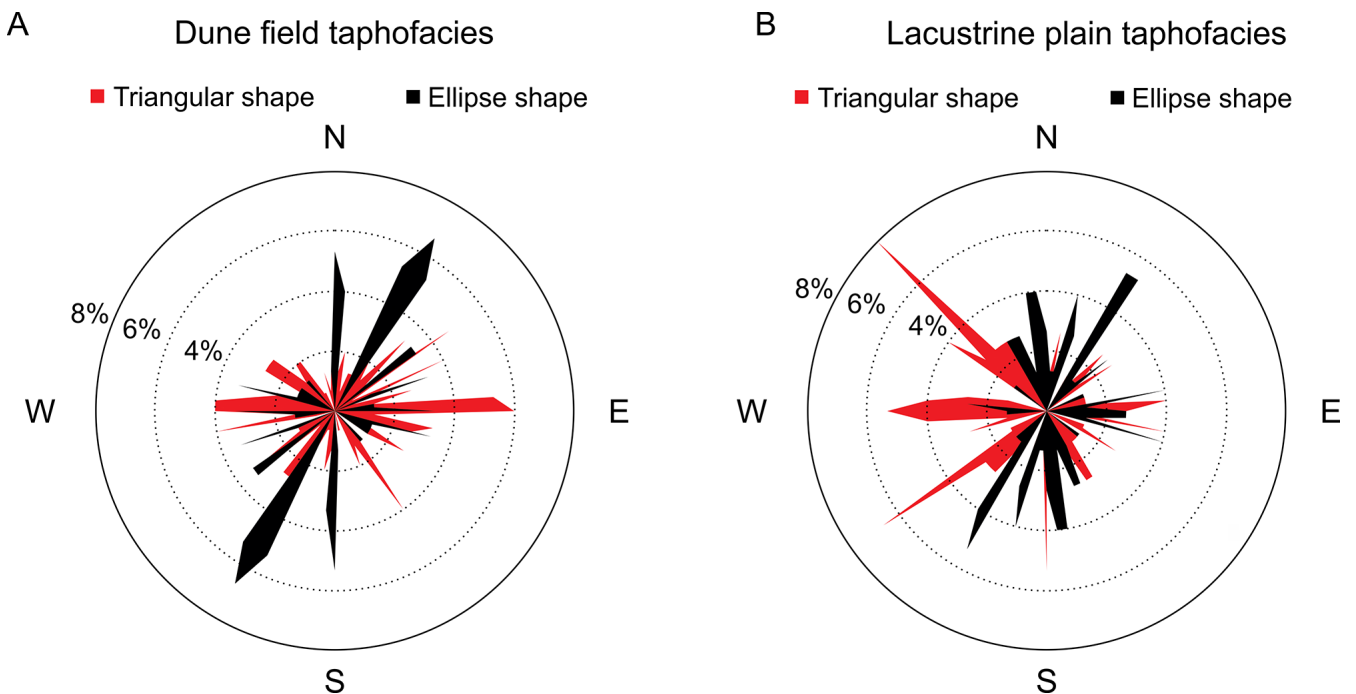


Figure 6. Graphic showing the relative frequency of hydrodynamic orientation of the long axis of bioclasts in plain view. Mirim Lake is located to the west, and the dune field is to the east of the compass rose. **A**, orientation of bioclasts in the Dune field taphofacies. **B**, orientation of bioclasts in the Lacustrine plain taphofacies.

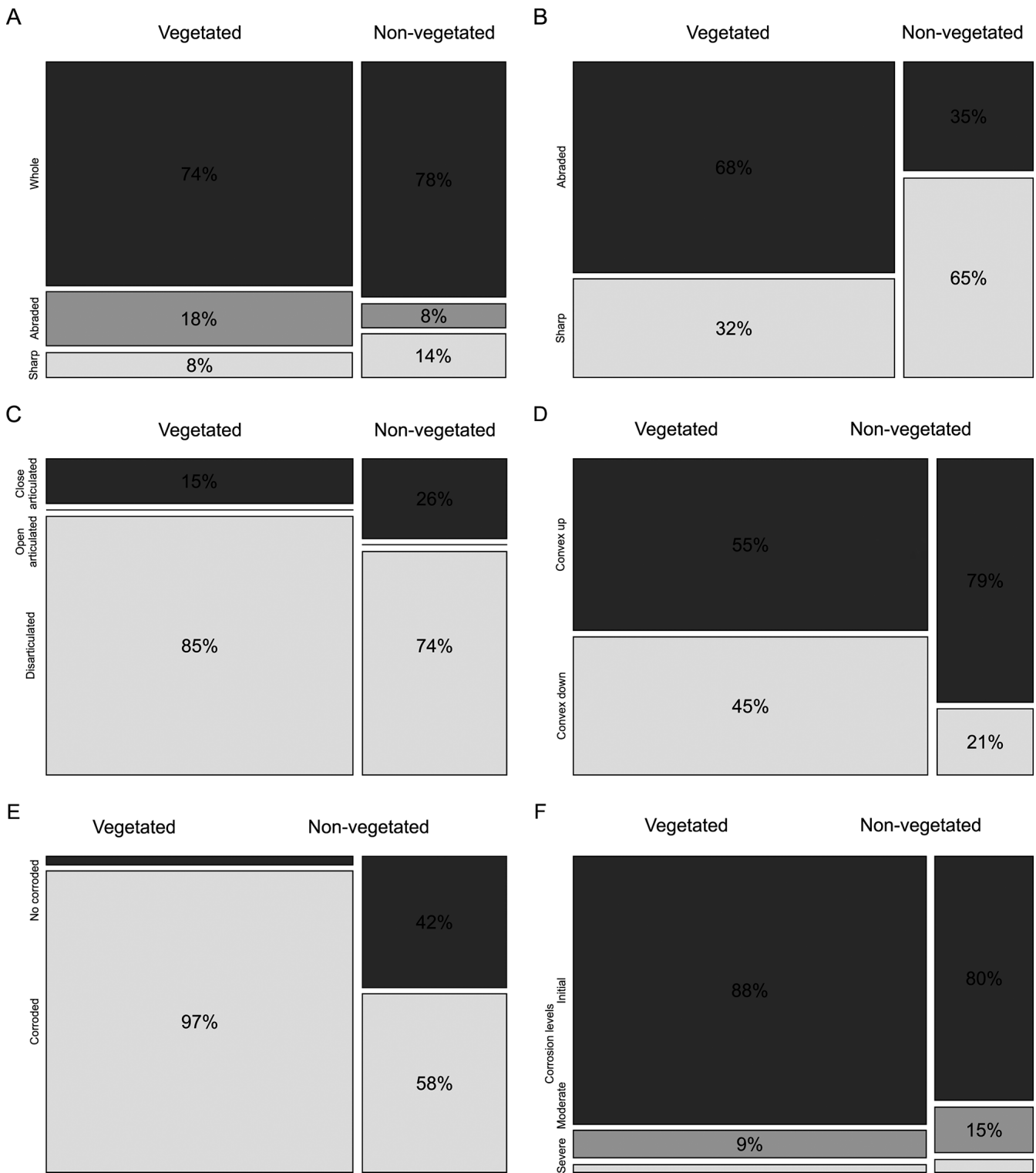


Figure 7. Mosaic plot showing the significantly different frequency ($p \leq 0.0001$) of taphonomic signatures between vegetated and non-vegetated sub-taphofacies. **A**, dominance of whole bioclasts in the dune field followed by the higher abrasion of bioclasts in the vegetated sub-taphofacies. **B**, frequency of abraded and sharp bioclasts considering only fragments. **C**, higher frequency of disarticulated valves than articulated ones to both sub-taphofacies of Mirim Lake. **D**, higher occurrence of hydrodynamic stable positioned valves only in the non-vegetated sub-taphofacies. **E**, higher occurrence of corroded bioclasts only in the vegetated sub-taphofacies. **F**, a similar proportion of corrosive damage between the two sub-taphofacies.

were corroded ($f = 98\%$), with 2744 ($f = 93\%$) categorized as initial, 169 ($f = 4\%$) as moderate, and 18 ($f = 1\%$) as severe corrosion levels (Figure 5D, Table 1). The ratio of corroded/non-corroded bioclasts is significant ($p < 0.0001$). Initial levels of corrosion are the most common ($p < 0.0001$) (Table 1).

DISCUSSION

The data of the Mirim Lake revealed that damaged bioclasts are frequent, with at least 42% ($n = 1,844$ of 4,333) fragmented and 94% showing different levels of corrosion (initial dissolution = 87%, moderate dissolution = 6%, severe dissolution = 1%). Of 1,844 fragments, 71% were classified as sharp-edged ($n = 1,312$) and abraded (29%, $n = 532$). Abrasion of bioclasts (rounding of their edges and surface wear) needs time for reworking and exposing them to abrasive elements (Driscoll, 1967; Meldahl & Flessa, 1990; Salamon *et al.*, 2020). Therefore, it is possible to infer that the bioclasts remained exposed to damaging conditions (mechanical, biological, and chemical) for different periods.

Considering the low energy gradient of lake environments, mechanical reworking is not expected to be the primary damaging agent (Cate & Evans, 1994). Nearly all bioclasts (94%) exhibit some degree of corrosion, resulting in the weakness of the valves and making them more susceptible to breaking. Furthermore, some bioclasts show signs of trampling (Figure 2D) that could be attributed to the presence of cattle grazing and local fishermen at the shore.

Corrosion levels vary from slight (initial = loss of luster and color) to severe damages (total deterioration of the affected zone of the valve, Figure 8). In one specimen of *Diplodon ellipticus*, it is possible to observe stains of dissolution (Figure 8D). At the same time, another has its pearly layer exposed due to severe dissolution (Figure 8B). Although the umbo is a thicker structure of the shell, some valves show the most accentuated damage in this portion (Figure 8A). A combined effect of corrosion and abrasion could have caused the complete loss of the umbo of the specimen illustrated in Figure 8A. Diverse factors and features (*e.g.*, taxon, size, weight) are involved in the corrosion rates (Flessa & Brown, 1983).

Despite the small number, the articulated bivalves provide information about the sedimentary dynamic of the lake. At least 7.5% of all bioclasts were closed-articulated, indicating brief exposure and no reworking after dying. The opening of the valves is relatively fast. It is due to the functional anatomy of the ligament that forces the aperture of the bivalve after the decay of the soft tissues (adductor muscle). Moreover, the disarticulation (partial or total) is directly related to the sedimentation rate and energy gradient (besides the oxygen content of the environment and the exposure time and reworking of the articulated skeleton) (Allen, 1990; Brett, 2003; Gendy *et al.*, 2015; Ilari *et al.*, 2015), which reinforces the hypotheses of brief exposure and no reworking.

Differences in the taphonomic signatures along the beach profile of Mirim Lake led to the recognition of two

taphofacies: the dune field taphofacies and lacustrine plain taphofacies.

Densely concentrated shell deposits, with a higher proportion of both whole (75%) and closed-articulated bivalves (18%) deposited in the front dune zone, characterize the field dune taphofacies. In addition, at least 16% of bioclasts did not exhibit loss of color or luster. Dense concentrations were only observed in the vegetated zones of the dune fields, suggesting that the higher accumulation of the shells may result from their trapping in the vegetation combined with a low sedimentation rate. On the other hand, the better preservation of bioclasts (*i.e.*, whole and articulated shells, preservation of color, and absence of corrosion signs) is usually attributed to low exposure in the taphonomic active zone (Meldahl & Flessa, 1990; Olszewski, 2004), which suggests that this shell assemblages probably represent recent deposits.

Some birds show a behavior known as avian prey-dropping behavior, which may produce concentrations of shell fragments (Maron, 1982; Cristol & Switzer, 1999; Switzer & Cristol, 1999). This behavior involves birds dropping the shells on hard ground to break them. However, the dune field at Mirim Lake is characterized by a soft surface that is inadequate for this behavior.

Concentrations of shells of *Corbicula fluminea* as artificial deposits made by fisherman activities have been described in Argentina (Labaut *et al.*, 2021). Despite the occurrence of fisherman activity in Mirim Lake, this hypothesis is discarded because the bioclasts that form the shell concentrations on the dune field show different sizes, which refutes the idea that they could be used as bait. Moreover, the shell deposits show sinuous geometry, suggesting wavy reworking. Therefore, it seems more plausible to consider that the bioclasts were transported during flood periods (when the level of the lake rises) and were deposited about 117 m away (Figures 1C–D) when the lake's level fell.

Flooding of lacustrine plain and front dunes in the dune field is a standard process in Mirim Lake, ranging from 2 to 3 m (Oliveira *et al.*, 2015). Since Mirim Lake has no connection to the sea, the floods are linked to the weather (seasonal rain and storms), while low-water periods are closely related to the use of the lake's water in the rice fields (Motta Marques *et al.*, 2002). A graphic summarizing the seasonal level variation of the Taim region over several decades can be found in Motta Marques *et al.* (2002).

Bivalve shells show good floatability and thus are easily transported (Lever *et al.*, 1964; Brenchley & Newall, 1970; Allen, 1984; Dent & Uhen, 1993). As a result, bioclasts would be deposited along the beach profile. Thus, it is plausible to infer the transport of bivalves to the front dunes during the maximum flooding periods and their subsequent trapping in the vegetation during the drought periods.

Wind-induced sediment dynamics are the primary process related to the transport of sand in dune environments (Tomazelli, 1993). Fast burials may result from wind-induced sediment dynamics, which would favor the preservation of bioclasts as observed here (whole and closed-articulated

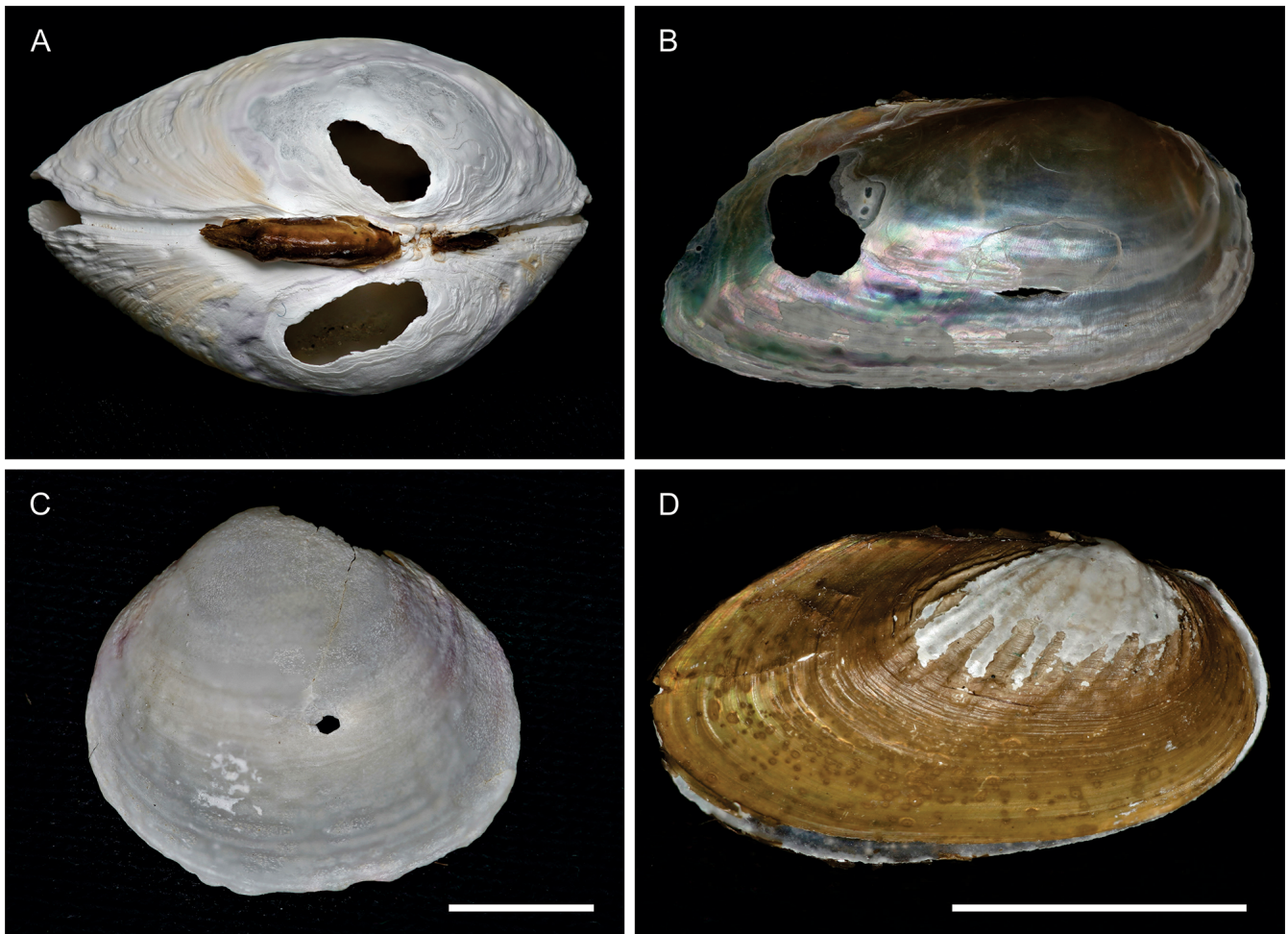


Figure 8. Different degrees of corrosion were observed in the bioclasts of Mirim Lake. **A**, closed-articulated specimen of *Corbicula* (ULVG 14292) showing intense surface corrosion resulting in the complete degradation of the umbo, loss of color, and formation of dissolution pits. **B**, severe dissolution damage on a *Diplodon* valve (ULVG 14305) (complete loss of the superficial layers and subsequent exposure of the pearly layer). **C**, a valve of *Corbicula* sp. (ULVG 14294) showing severe corrosion (loss of color, formation of dissolution pits, and partial degradation of the umbo). **D**, a specimen of *Diplodon ellipticus* (ULVG 14304) showing dissolution stains and peeled umbo (initial level of corrosion). Scale bars: A–B = not scale; C–D = 10 mm.

bivalves). Furthermore, sharp fragments are more abundant in non-vegetated than vegetated areas of the dune fields, which suggests that the bioclasts were differently affected in each zone. In summary, there is a difference in the time exposure of bioclasts in each dune field area.

The lacustrine plain taphofacies is characterized by shell accumulations varying from loosely concentrated to scattered. They are arranged as wavy, laterally extended deposits following the parallel line of the lake. Distinct characteristics of lacustrine plain taphofacies are the higher proportion of disarticulated and open-articulated bivalves, sharp fragments, and corroded bioclasts.

Despite the higher frequency of closed-articulated bivalves recorded on the dune field (18.7%, Table 1), the occurrence of open-articulated bivalves was higher in the lacustrine plain (1.8%) (Figure 2C, Table 1). The bivalves were observed in both convex down and convex up positions (Figure 2C). Due to the instability of the convex down orientation, they are quickly turned over to convex up by currents (Allen, 1990; Brett, 2003). In this sense, open-articulated bivalves oriented in an unstable hydrodynamic position (*i.e.*, convex down,

Figure 2C) may open after being stranded concomitantly with the fall of the water level. Open-articulated bivalves in a stable hydrodynamic position (Figures 2C and 3C) suggest that lake currents can capsized them.

Although previous works have already demonstrated that convex-down valves are frequent in tidal flats during periods of fair weather (Brenchley & Newall, 1970; Allen, 1984; Dent & Uhen, 1993), a relationship between the occurrence of convex-down open-articulated bivalves and predator activities cannot be discarded.

The sinuosity of DA margins (Figure 3A) is evidence of the action of waves that reworked the shells. At the same time, the abundance of sharp fragments points to the low residence time of these bioclasts in contact with abrasive elements. Studies on shallow lakes (*e.g.*, Bengtsson & Hellström, 1992; Lövstedt & Bengtsson, 2008) have demonstrated that waves induced by winds are common, and the waves and currents generated during higher kinetic events such as storms can resuspend and transport the sediment of the whole lake. Higher water turbulence due to constant and strong winds associated with a shallow condition is attributed to Mirim

Lake (Goulart & Saito, 2012). In this sense, the reworking of bioclasts by wind-induced waves can be expected on the lake shore.

CONCLUSIONS

Distinct taphonomic signatures were observed in the death assemblages along all beach profiles from the dune field to the lacustrine plain. This led to recognizing two taphofacies: dune field and lacustrine plain taphofacies.

Flood events and wind-induced sediment dynamics were associated with the genesis of the death assemblages observed in the dune field taphofacies, which resulted in a lower reworking of bioclasts (higher proportion of closed-articulated bivalves) and a higher abundance of abraded fragments, which highlights their exposure to abrasive agents.

A higher frequency of abraded and a low number of bioclasts showing no signs of corrosion was observed in the vegetated areas of the dune fields. In contrast, opposite results were observed in non-vegetated dunes, allowing to classify these as sub-taphofacies from the dune field taphofacies.

Wind-induced waves and low exposure to abrasive agents were conditions attributed to the lacustrine plain, evidenced by the wavy shape of death assemblages deposited on the shore and the abundance of sharp-edged fragments.

Finally, three sedimentary dynamics were recognized. The first two correspond to flooding and wind-induced sediment dynamics linked to the genesis of death assemblages in the dune field. The third corresponds to wind-induced wave dynamics related to the genesis of death assemblages in the lacustrine plain.

ACKNOWLEDGMENTS

The author is grateful to CAPES – Coordenação de Aperfeiçoamento de Pessoal de Nível Superior PNPd grant, FAPERGS for grant 21/2551-0002035-0, Rômulo Cenci for helping with photographs. I am very grateful to the reviewers for their contributions to the best version of this work.

REFERENCES

- Allen, J.R.L. 1984. Experiments on the terminal fall of the valves of bivalve mollusks loaded with sand trapped from a dispersion. *Sedimentary Geology*, **39**:197–209. doi:10.1016/0037-0738(84)90050-2
- Allen, J.R.L. 1990. Transport-hydrodynamics: shells. In: D.E.G. Briggs & P.C. Crowther (eds.) *Palaeobiology: a synthesis*, Blackwell Science, p. 227–229.
- Barboza, E.G.; Rosa, M.L.C.C. & Ayup-Zouain, R.N. 2008. Cronoestratigrafia da Baía de Pelotas: uma revisão das seqüências deposicionais. *Gravel*, **6**:125–138.
- Behrensmeier, A.K.; Fürsich, F.T.; Gastaldo, R.A.; Kidwell, S.M.; Kosnik, M.A.; Kowalewski, M.; Plotnick, R.E.; Rogers, R.R. & Alroy, J. 2005. Are the most durable shelly taxa also the most common in the marine fossil record? *Paleobiology*, **31**:607–623. doi:10.1666/04023.1
- Bengtsson, L. & Hellström, T. 1992. Wind-induced resuspension in a small shallow lake. *Hydrobiologia*, **241**:163–172. doi:10.1007/BF00028639
- Best, M.M.R. & Kidwell, S.M. 2000a. Bivalve taphonomy in tropical mixed siliciclastic-carbonate settings. I. Environmental variation in shell condition. *Paleobiology*, **26**:80–102. doi:10.1666/0094-8373(2000)026<0080:BTITMS>2.0.CO;2
- Best, M.M.R. & Kidwell, S.M. 2000b. Bivalve taphonomy in tropical mixed siliciclastic-carbonate settings. II. Effect of bivalve life habits and shell types. *Paleobiology*, **26**:103–115. doi:10.1666/0094-8373(2000)026<0103:BTITMS>2.0.CO;2
- Brenchley, P.J. & Newall, G. 1970. Flume experiments on the orientation and transport of models and shell valves. *Palaeogeography, Palaeoclimatology, Palaeoecology*, **7**:185–220. doi:10.1016/0031-0182(70)90093-3
- Brett, C.E. 2003. Taphonomy: sedimentological implications of fossil preservation. In: G.V. Middleton (ed.) *Encyclopedia of sediments and sedimentary rocks*, Springer, p. 723–729.
- Brett, C.E. & Baird, G.C. 1986. Comparative taphonomy: a key to paleoenvironmental interpretation based on fossil preservation. *Palaios*, **1**:207–227. doi:10.2307/3514686
- Cate, A.S. & Evans, I. 1994. Taphonomic Significance of the Biomechanical Fragmentation of Live Molluscan Shell Material by a Bottom-Feeding Fish (*Pogonias cromis*) in Texas Coastal Bays. *Palaios*, **9**:254–274. doi:10.2307/3515201
- Cristol, D.A. & Switzer, P.V. 1999. Avian prey-dropping behavior. II. American crows and walnuts. *Behavioral Ecology*, **10**:220–226. doi:10.1093/beheco/10.3.220
- De Francesco, C.G. & Hassan, G.S. 2008. Dominance of reworked fossil shells in modern estuarine environments: implications for paleoenvironmental reconstructions based on biological remains. *Palaios*, **23**:14–23. doi:10.2110/palo.2006.p06-124r
- Dent, S.R. & Uhen, M.D. 1993. Tidal Reorientation and Transport of Recent Bivalves on a Temperate Tidal Flat, Northwestern U.S. *Palaios*, **8**:244–249. doi:10.2307/3515147
- Dietl, G.P. 2016. Brave new world of Conservation Paleobiology. *Frontiers in Ecology and Evolution*, **4**:10–12. doi:10.3389/fevo.2016.00021
- Dietl, G.P. & Flessa, K.W. 2011. Conservation paleobiology: putting the dead to work. *Trends in Ecology & Evolution*, **26**:30–37. doi:10.1016/j.tree.2010.09.010
- Driscoll, E.G. 1967. Experimental field study of shell abrasion. *Journal of Sedimentary Petrology*, **37**:1117–1123. doi:10.1306/74D71843-2B21-11D7-8648000102C1865D
- Flessa, K.W. & Brown, T.J. 1983. Selective solution of macroinvertebrate calcareous hard parts: a laboratory study. *Lethaia*, **16**:193–205. doi:10.1111/j.1502-3931.1983.tb00654.x
- Fürsich, F.T. & Kirkland, J.I. 1986. Biostratigraphy and Paleocology of a Cretaceous Brackish Lagoon. *Palaios*, **1**:543–560. doi:10.2307/3514706
- Fürsich, F.T. & Oschmann, W. 1993. Shell beds as tools in basin analysis: the Jurassic of Kachchh, western India. *Journal of the Geological Society*, **150**:169–185. doi:10.1144/gsjgs.150.1.0169
- Fürsich, F.T.; Pan, Y.; Wilmsen, M. & Majidifard, M.R. 2016. Biofacies, taphonomy, and paleobiogeography of the Kamar-e-Mehdi Formation of east-central Iran, a Middle to Upper Jurassic shelf lagoon deposit. *Facies*, **62**:1–23. doi:10.1007/s10347-015-0452-6

- Gendy, A.E.; Al-Farraj, S. & El-Hedeny, M. 2015. Taphonomic Signatures on some intertidal molluscan shells from Tarut Bay (Arabian Gulf, Saudi Arabia). *Pakistan Journal of Zoology*, **47**:125–132.
- Ghilardi, R.P. & Simões, M.G. 2002. Foram os Bivalves do Grupo Passa Dois (Exclusive Formação Rio do Rasto), Neopermiano, Invertebrados Tipicamente Dulcícolas? *Pesquisas em Geociências*, **29**:83–95. doi:10.22456/1807-9806.19600
- Goulart, F.F. & Saito, C.H. 2012. Modelagem dos impactos ecológicos do projeto hidroviário da Lagoa Mirim (Brasil-Uruguai), baseada em raciocínio qualitativo. *Brazilian Journal of Aquatic Science and Technology*, **16**:19–31.
- Ilarri, M.I.; Souza, A.T. & Sousa, R. 2015. Contrasting decay rates of freshwater bivalves' shells: Aquatic versus terrestrial habitats. *Limnologia*, **51**:8–14. doi:10.1016/j.limno.2014.10.002
- Kidwell, S.M. 1986. Taphonomic feedback in Miocene assemblages: testing the role of dead hardparts in benthic communities. *Palaios*, **1**:239–255. doi:10.2307/3514688
- Kidwell, S.M. 1998. Time-averaging in the marine fossil record: overview of strategies and uncertainties. *Geobios*, **30**:977–995. doi:10.1016/S0016-6995(97)80219-7
- Kidwell, S.M. 2001. Preservation of species abundance in marine death assemblages. *Science*, **294**:1091–1094. doi:10.1126/science.1064539
- Kidwell, S.M. 2007. Discordance between living and death assemblages as evidence for anthropogenic ecological change. *Proceedings of the National Academy of Sciences*, **104**:17701–17706. doi:10.1073/pnas.0707194104
- Kidwell, S.M. 2008. Ecological fidelity of open marine molluscan death assemblages: effects of post-mortem transportation, shelf health, and taphonomic inertia. *Lethaia*, **41**:199–217. doi:10.1111/j.1502-3931.2007.00050.x
- Kidwell, S.M. 2013. Time-averaging and fidelity of modern death assemblages: building a taphonomic foundation for conservation palaeobiology. *Palaeontology*, **56**:487–522. doi:10.1111/pala.12042
- Kidwell, S.M.; Fürsich, F.T. & Aigner, T. 1986. Conceptual framework for the analysis and classification of fossil concentrations. *Palaios*, **1**:228–238. doi:10.2307/3514687
- Kidwell, S.M. & Jablonski, D. 1983. Taphonomic feedback ecological consequences of shell accumulation. In: M.J.S. Tevesz (ed.) *Biotic interactions in Recent and fossil benthic communities*, Springer, p. 195–235. doi:10.1007/978-1-4757-0740-3_5
- Kowalewski, M. 1999. Actupaleontology: the strength of its limitations. *Acta Palaeontologica Polonica*, **4**:452–454.
- Kowalewski, M.; Flessa, K.W. & Aggen, J.A. 1994. Taphofacies analysis of Recent shelly cheniers (Beach Ridges), Northeastern Baja California, Mexico. *Facies*, **31**:209–241. doi:10.1007/BF02536940
- Labaut, Y.; Macchi, P.A.; Archuby, F.M. & Darringran, G.A. 2021. Pesca con carnada viva como vector dispersante de la invasión de la almeja asiática *Corbicula fluminea* en Patagonia, Argentina. In: SIMPOSIO INTERNACIONAL AGUAS CONTINENTALES DE LAS AMÉRICAS RESTAURACIÓN Y CONSERVACIÓN DE LOS ECOSISTEMAS COM ENFOQUE PARTICIPATIVO, 3, 2021. *Resumos*, Panajachel, Universidad del Valle de Guatemala.
- Lever, J.; Bosch, M.; Cook, H.; Dijk, T.; Thiadens, A.J.H. & Thijssen, R. 1964. Quantitative beach research. III. An experiment with artificial valves of *Donax vittatus*. *Netherlands Journal of Sea Research*, **2**:458–492. doi:10.1016/0077-7579(64)90003-1
- Lopes, R.P. & Buchmann, F.S. de C. 2008. Comparação tafonômica entre duas concentrações fossilíferas (*shell beds*) da Planície Costeira do Rio Grande do Sul, Brasil. *Gaea*, **4**:65–77. doi:10.4013/gaea.20082.03
- Lopes, R.P.; Pereira, J.C.; Kinoshita, A.; Molleberg, M.; Barbosa, F. & Baffa, O. 2020. Geological and taphonomic significance of electron spin resonance (ESR) ages of Middle-Late Pleistocene marine shells from barrier-lagoon systems of Southern Brazil. *Journal of South American Earth Sciences*, **101**:102605. doi:10.1016/j.jsames.2020.102605
- Lopes, R.P. et al. 2021. Late Pleistocene-Holocene fossils from Mirim Lake, southern Brazil, and their paleoenvironmental significance: II – Mollusks. *Journal of South American Earth Sciences*, **112**:103546. doi:10.1016/j.jsames.2021.103546
- Lövstedt, C.B. & Bengtsson, L. 2008. The role of non-prevailing wind direction on resuspension and redistribution of sediments in a shallow lake. *Aquatic Sciences*, **70**:304–313. doi:10.1007/s00027-008-8047-8
- Maron, J.L. 1982. Shell-Dropping Behavior of Western Gulls (*Larus occidentalis*). *The Auk*, **99**:565–569.
- Meldahl, K.H. 1987. Sedimentologic and taphonomic implications of biogenic stratification. *Palaios*, **2**:350. doi:10.2307/3514760
- Meldahl, K.H. & Flessa, K.W. 1990. Taphonomic pathways and comparative biofacies and taphofacies in a Recent intertidal/shallow shelf environment. *Lethaia*, **23**:43–60. doi:10.1111/j.1502-3931.1990.tb01780.x
- Motta Marques, D.M.L.; Tucci, C.; Calazans, C.; Callegaro, V.L.M. & Villanueva, A. 2002. O Sistema Hidrológico do Taim – site 7. In: U. Seeliger; C.V. Cordazzo & F. Barbosa (eds.) *Os Sites e o programa Brasileiro de pesquisas ecológicas de longa duração*, MCT-CNPq, p. 125–144.
- Oliveira, H.A.; Fernandes, E.H.L.; Möller Jr., O.O. & Collares, G.L. 2015. Processos hidrológicos e hidrodinâmicos da Lagoa Mirim. *Revista Brasileira de Recursos Hídricos*, **20**:34–45. doi:10.21168/rbrh.v20n1.p34-45
- Olszewski, T. 2004. Modeling the influence of taphonomic destruction, reworking, and burial on time-averaging in fossil accumulations. *Palaios*, **19**:39–50. doi:10.1669/0883-1351(2004)019<0039:MTIOTD>2.0.CO;2
- Ritter, M.N.; Erthal, F. & Coimbra, J.C. 2013. Taphonomic signatures in molluscan fossil assemblages from the Holocene lagoon system in the northern part of the coastal plain, Rio Grande do Sul State, Brazil. *Quaternary International*, **305**:5–14. doi:10.1016/j.quaint.2013.03.013
- Rosa, M.L.C.; Barboza, E.G.; Abreu, V.S.; Tomazelli, L.J. & Dillenburg, S.R. 2017. High-frequency sequences in the Quaternary of Pelotas Basin (coastal plain): a record of degradational stacking as a function of longer-term base-level fall. *Brazilian Journal of Geology*, **47**:183–207. doi:10.1590/2317-4889201720160138
- Salamon, M.A.; Brachaniec, T. & Gorzelak, P. 2020. Durophagous fish predation traces versus tumbling-induced shell damage—a paleobiological perspective. *Palaios*, **35**:37–47. doi:10.2110/palo.2019.091
- Speyer, S.E. & Brett, C.E. 1986. Trilobite taphonomy and Middle Devonian taphofacies. *Palaios*, **1**:312–327. doi:10.2307/3514694
- Speyer, S.E. & Brett, C.E. 1988. Taphofacies models for epeiric sea environments: Middle Paleozoic examples. *Palaeogeography, Palaeoclimatology, Palaeoecology*, **63**:225–262. doi:10.1016/0031-0182(88)90098-3

- Switzer, P.V. & Cristol, D.A. 1999. Avian prey-dropping behavior. I. The effects of prey characteristics and prey loss. *Behavioral Ecology*, **10**:213–219. doi:10.1093/beheco/10.3.213
- Tomazelli, L.J. 1993. O Regime dos ventos e a taxa de migração das dunas eólicas costeiras do Rio Grande do Sul, Brasil. *Pesquisas em Geociências*, **20**:18–26. doi:10.22456/1807-9806.21278
- Tomazelli, L.J. & Villwock, J.A. 2000. O Cenozóico Costeiro do Rio Grande do Sul. In: M. Holz & L.F. de Ros (eds.) *Geologia do Rio Grande Do Sul*, p. 375–406.
- Tomazelli, L.J. & Villwock, J.A. 2005. Mapeamento geológico de planícies costeiras: o exemplo da costa do Rio Grande do Sul. *Gravel*, **3**:109–115.
- Tsolakos, K.; Katselis, G. & Theodorou, J.A. 2021. Taphonomy of mass mollusc shell accumulation at Amvrakikos Gulf lagoon complex sandy barriers (NW Greece). *Oceanologia*, **63**:179–193. doi:10.1016/j.oceano.2020.11.004
- Valentini, M.H.K. et al. 2020. Monitoring and identification of pollutant groups of the Lagoa Mirim. *Revista Ibero-Americana de Ciências Ambientais*, **11**:227–235. doi:10.6008/CBPC2179-6858.2020.004.0020
- Villwock, J.A. & Tomazelli, L.J. 1995. Geologia Costeira do Rio Grande do Sul. *Notas Técnicas*, **8**:1–45.
- Weber, K. & Zuschin, M. 2013. Delta-associated molluscan life and death assemblages in the northern Adriatic Sea: Implications for paleoecology, regional diversity and conservation. *Palaeogeography, Palaeoclimatology, Palaeoecology*, **370**:77–91. doi:10.1016/j.palaeo.2012.11.021
- Zar, J.H. 2010. *Biostatistical analysis*. 5th ed. Pearson, 960 p.
- Zuschin, M. & Ebner, C. 2015. Compositional fidelity of death assemblages from a coral reef-associated tidal-flat and shallow subtidal lagoon in the Northern Red Sea. *Palaios*, **30**:181–191. doi:10.2110/palo.2014.032

Received in 16 February, 2023; accepted in 20 November, 2023.